Modeling Spatiotemporal Armed Conflict Dynamics via Physics-Informed Diffusion

Jingtian Hu [1 †], Hao Sha [2 †], Pengfei Tian [3 †], Yue He [4], Chong Chen [1], Fan Yang [5], Peng Cui [4]

[1]Department of International Relations, Tsinghua University;
[2]Xingjian College, Tsinghua University;
[3]Qiuzhen College, Tsinghua University;
[4]Department of Computer Science and Technology, Tsinghua University;
[5]YAU Mathematical Science Center, Tsinghua University

AI4SS Workshop, May 2025

Predicting armed conflict: Time to adjust our expectations? (*Science*)

> *Therefore, the challenge for the field is to find the right balance between the inherent complexity of the social and political world and the associated limitations on our ability to accurately forecast political violence. Within a limited spatiotemporal radius, policy-relevant prediction is feasible and potentially extremely useful.*

(Cederman and Weidmann, 2017), *Science*

Identifying attacks in the Russia Ukraine conflict (*Nature*)

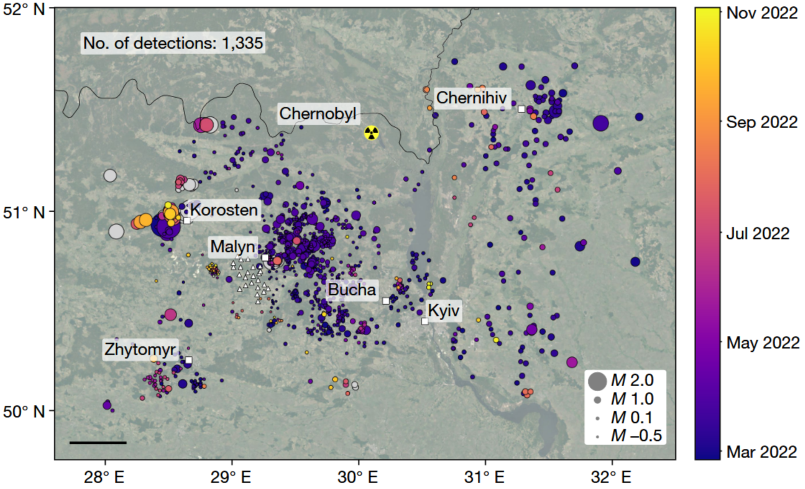

Figure 1: Map of automatic seismic detections in 2022 (Dando et al., 2023).

Gap: Accuracy-Interpretability Trade-off?

Traditional Machine Learning ✘ Oversimplify!

- **ViEWS**: Forecasting at least 1 BRD per GRID-month (Hegre et al., 2019, 2021, 2017)
- Simplistic Proxies - lagged binary variables (Muchlinski et al., 2016; Wang, 2019)

Spatiotemporal Deep Learning ✘ Black Box!

- **Models**: RNN/LSTM/GCN/ConvLSTM/STGCN (Brandt et al., 2022; Chadefaux, 2022; Hegre et al., 2022; Lindholm et al., 2022; Radford, 2022)

Physics-Informed Deep Learning ✓

- **Example**: Nonlinear forecasting for extreme precipitation events (Zhang et al., 2023)
- "Diffusion, relocation, heterogeneous escalation" (Zammit-Mangion et al., 2012)

Why Physics-Informed? Accuracy (36.4% → 56.7%)

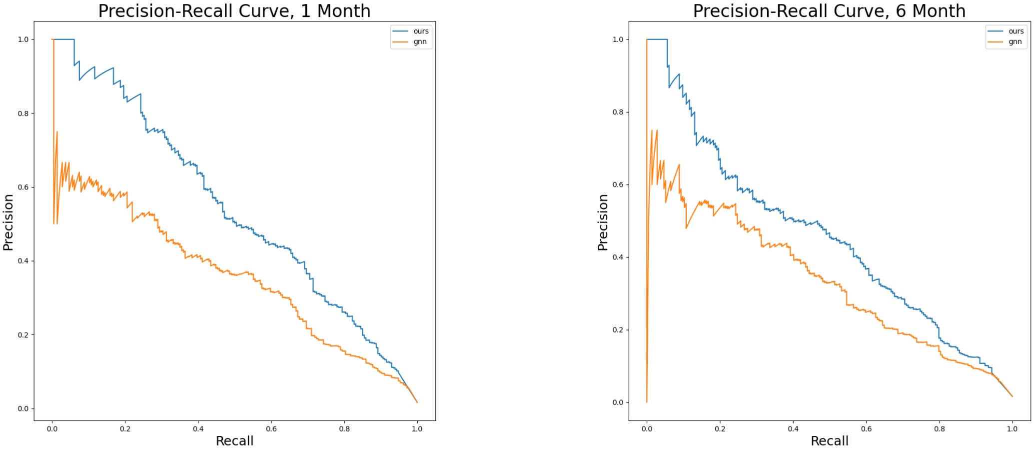

Figure 2: ConflictNet significantly improves PR performance compared to ViEWS.

Why Physics-Informed? Interpretability

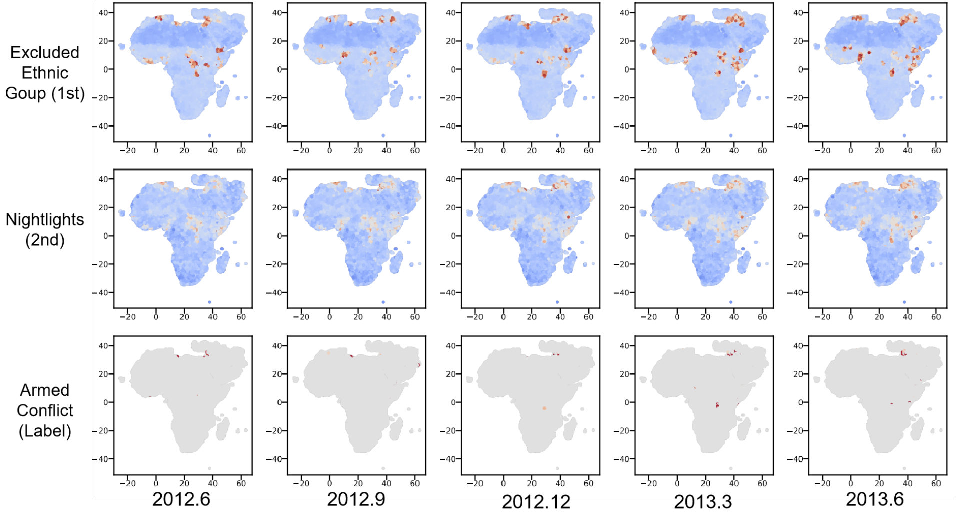

Figure 3: Feature Importance in Modeling Armed Conflict Spreading

The Physics-Informed Modeling

Motivation: Diffusion As Falling Balls

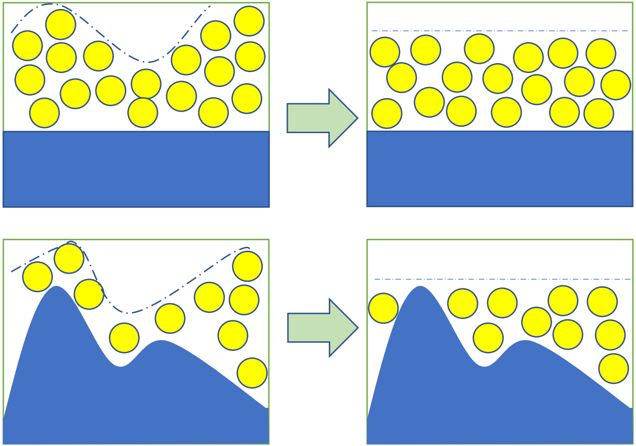

Figure 4: Illustration of feature diffusion. In the presence of a spatial potential field $\phi(\mathbf{x})$, diffusion proceeds until the gradient force $\nabla \mathbf{u}(\mathbf{x}, \mathbf{t})$ balances the external force $-\nabla \phi(\mathbf{x})$, reaching equilibrium.

Motivation Check: Regression to the Local Mean

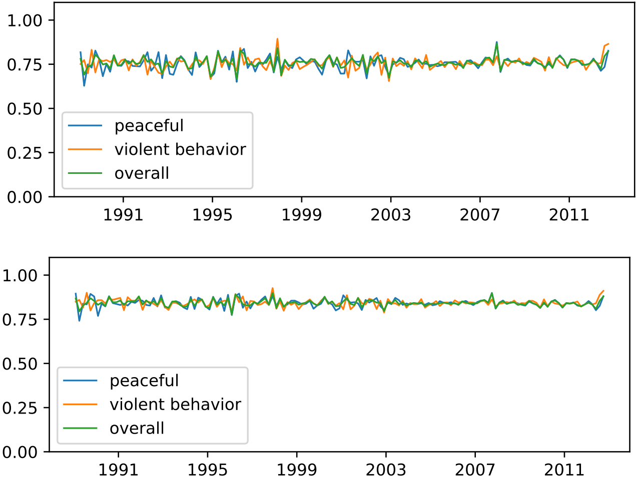

Figure 5: Share of grid cells where next-step feature values move toward the local mean.

Overall Settings of Armed Conflict Spreading

At each location $\mathbf{x}$ and time t, let $\mathbf{s}(\mathbf{x}, t) \in \mathbb{R}^l$ denote the density of l types of conflict-driving factors (Bertozzi et al., 2010; Epstein, 2002; Helbing, 2001; Porter and Gleeson, 2016).

The overall transfer dynamics of conflict factors are thus expressed as:

$$\frac{\partial \mathbf{s}}{\partial t} = \mathbf{p} \odot \frac{\partial \mathbf{u}}{\partial t} + (1 - \mathbf{p}) \odot \frac{\partial \mathbf{w}}{\partial t} + \mathbf{q}(\mathbf{x}, t)$$

- $\mathbf{u}$: local diffusion (e.g. unrest spills to neighbors)
- $\mathbf{w}$: rigid-body movement (e.g. group relocation)
- $\mathbf{q}$: source/sink (e.g. new protests or de-escalation)
- $\mathbf{p}$: controls mode mixing at each point

Model (1): Distribution

Under a spatial potential field $\phi(\mathbf{x})$, conflict factors settle following the **Boltzmann distribution** (Galam, 1997; Nicolas and Hassan, 2023; Orlova, 2024):

Assumption 1: Boltzmann Equilibrium

$$\pi(\mathbf{x}) \propto \exp(-\beta\phi(\mathbf{x})), \tag{1}$$

- $\phi(\mathbf{x})$: encodes spatial heterogeneity (strategic value, borders)(O'Loughlin et al., 2010)
- β: reflects sensitivity or propensity toward violence: higher β means sharper concentration.

Proposition 1: Directional Transition

In a potential field $\phi(\mathbf{x})$, a probability density $P\phi(\mathbf{x},\mathbf{r},\Delta t)$ that a conflict factor moves from location $\mathbf{x}$ to $\mathbf{x}+\mathbf{r}$ within time Δt is given by:

$$P\phi(\mathbf{x},\mathbf{r},\Delta t) = \frac{1}{Z}\exp\left[-\frac{\beta}{2}\{\phi(\mathbf{x}+\mathbf{r}) - \phi(\mathbf{x})\}\right] P(\|\mathbf{r}\|,\Delta t), \tag{2}$$

Model (2): Moment

Conflict spread is not instantaneous: mobilization is limited by logistical, infrastructural, and organizational constraints(Brockmann and Helbing, 2013; Holmes, 1993).

Assumption 2: Local Transition Scaling (Krapivsky et al., 2010)

$$\int_{\mathbb{R}^2} \|\mathbf{r}\|^2 P(\|\mathbf{r}\|, \Delta t) d\mathbf{r} \asymp \Delta t, \quad \int_{\mathbb{R}^2} \|\mathbf{r}\|^3 P(\|\mathbf{r}\|, \Delta t) d\mathbf{r} = o(\Delta t). \tag{3}$$

Proposition 2: Covariance structure

Under Assumption 2 and Proposition 1, there exists a constant $D > 0$ such that:

$$(2Z\Delta t)^{-1} \int_{\mathbb{R}^2} \mathbf{r}\mathbf{r}^{\mathrm{T}} P(\|\mathbf{r}\|, \Delta t) d\mathbf{r} = D\mathbf{I}_2. \tag{4}$$

Interpretation: Diffusion coefficient D captures organizational difficulty.

Higher D: weaker group control, greater individual autonomy, and increased difficulty in sustaining coordinated insurgent action.

Model (3): Diffusion Equation

Assumption 3: Coupling of Transitions (Couzin et al., 2005)

There exists a constant matrix $\boldsymbol{\xi}$ where $\xi_{ii} = 0$ for all i, such that a transition in u_j proportionally induces a transition in u_i, scaled by the coupling coefficient ξ_{ji}. Then:

$$\mathbf{u}(\mathbf{x}, t + \Delta t) = \int \mathbf{P}\phi \odot \mathbf{u}(\mathbf{x} - \mathbf{r}, t)\, d\mathbf{r} - \boldsymbol{\xi}^{\top}\mathbf{J}(\mathbf{x}, t) \tag{5}$$

Theorem 3: Diffusion Equation

The transfer equation of $\mathbf{u}(\mathbf{x}, t)$ is given by:

$$\frac{\partial \mathbf{u}}{\partial t} = (\boldsymbol{\xi}^{\top} + \mathbf{I}_l)\left[\mathbf{D} \odot (\nabla_{\mathbf{x}} \cdot \nabla_{\mathbf{x}}\mathbf{u}) + \mathbf{D} \odot \boldsymbol{\beta} \odot \{(\nabla_{\mathbf{x}}\mathbf{u})^{\top}\nabla_{\mathbf{x}}\phi\}\right], \tag{6}$$

where $\nabla_{\mathbf{x}}\mathbf{u} = [\nabla_{\mathbf{x}}u_1, \ldots, \nabla_{\mathbf{x}}u_l]$ and $\nabla_{\mathbf{x}} \cdot \nabla_{\mathbf{x}}\mathbf{u} = (\nabla_{\mathbf{x}} \cdot \nabla_{\mathbf{x}}u_1, \ldots, \nabla_{\mathbf{x}} \cdot \nabla_{\mathbf{x}}u_l)^{\top}$.

Illustration of Diffusion With Parameters

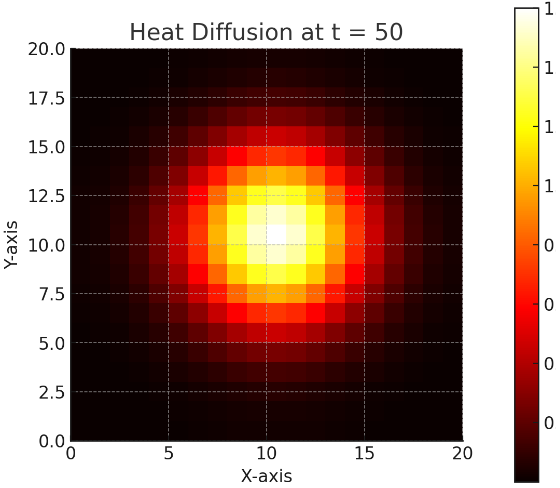

Figure 6: Plain Context

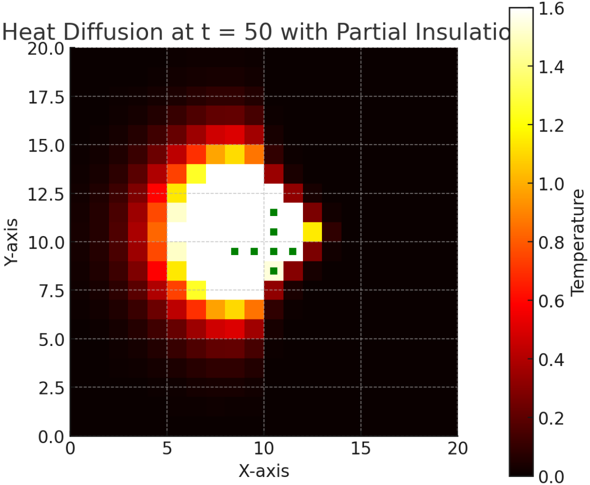

Figure 7: Considering D and ϕ

Summary: Physics-Informed Modeling

Diffusion	$\frac{\partial \mathbf{u}}{\partial t} = (\boldsymbol{\xi}^\top + \mathbf{I}_l)\left[\mathbf{D} \odot (\nabla_\mathbf{x} \cdot \nabla_\mathbf{x}\mathbf{u}) \quad + \mathbf{D} \odot \boldsymbol{\beta} \odot \left\{(\nabla_\mathbf{x}\mathbf{u})^\top \nabla_\mathbf{x}\phi\right\}\right];$
Relocation	$\xi^\top \mu \nabla \phi = \mathbf{u} \odot \mathbf{a}, \mathbf{X} = \int \mathbf{v}^0\, dt + \frac{1}{2}\mathbf{a}\,(dt)^2;$
Combination	$\frac{\partial \mathbf{s}}{\partial t} = \mathbf{p} \odot \frac{\partial \mathbf{u}}{\partial t} + (1 - \mathbf{p}) \odot \frac{\partial \mathbf{w}}{\partial t} + \mathbf{q}(\mathbf{x}, t)$

Physical Meaning

- t Time step
- D Viscosity
- β Mobility
- ϕ Potential field

Social Interpretation

- t 5 time steps per month
- D **Aggregation**: difficulty of collective action
- β **Violence Tendency**: willingness to engage in violence
- ϕ **Strategic Value**: attractiveness to insurgents

Embedded in Deep Learning

The Framework of ConflictNet

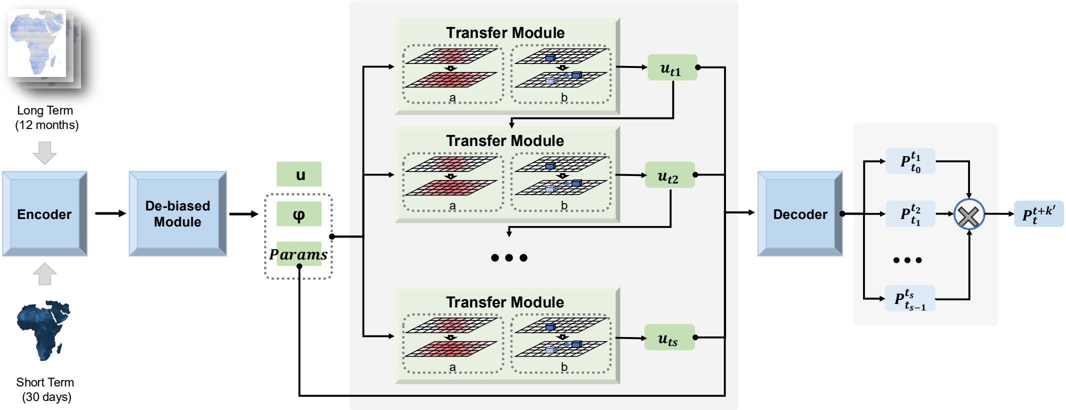

Figure 8: ConflictNet architecture. Encoder extracts features; de-bias module debiases and estimates PDE parameters; transfer module simulates dynamics and predicts conflict.

Data Sources and Granularity

Conflict & Contextual Data

- **UCDP-GED** – Armed conflict events
- **ACLED** – Political violence and protest
- **PRIO-GRID** – Subnational grid
- **World Bank WDI** – Development indicators
- **Ethnic Exclusion** (Cederman, 2010)
- **Demographics** (Lutz et al. 2007)
- **V-Dem** – Institutional quality

Spatiotemporal Granularity

Temporal:

- Harmonized to **monthly** (1990 to 2020)

Spatial:

- Country-level and PRIO-GRID $(0.5^\circ \times 0.5^\circ)$
- $\sim$13,000 cells $\times$370 months $\Rightarrow$ **4.78M observations**

Data Visualization

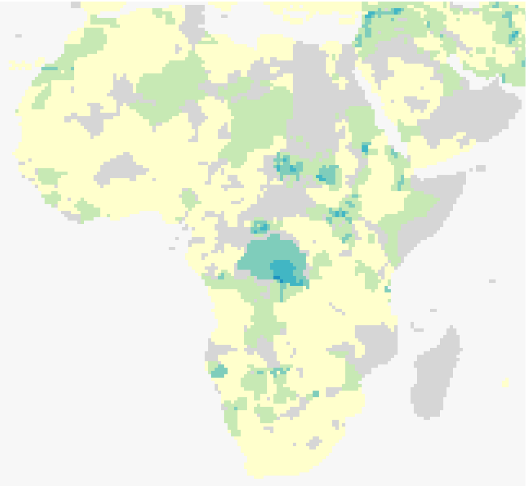

Figure 9: Excluded Ethnic Groups (2013.3)

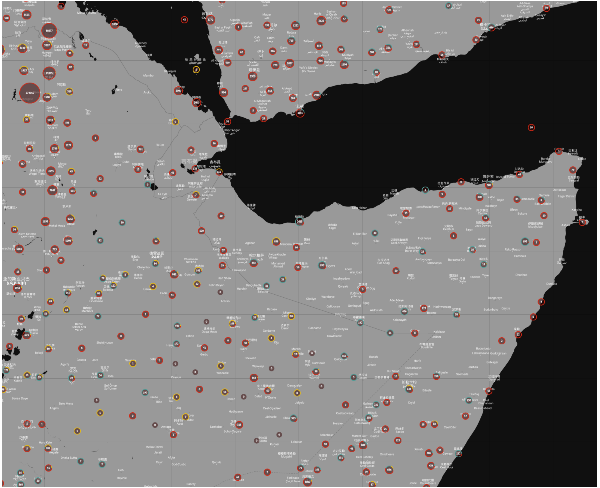

Figure 10: Intrastate Armed Conflict (UCDP)

Evaluation Metrics: Classification Performance

ROC-AUC (Receiver Operating Characteristic Curve)

- **TPR (Recall)**: $\frac{TP}{TP+FN}$
  True positive rate (sensitivity)
- **TNR**: $\frac{TN}{TN+FP}$
  True negative rate (specificity)
- Measures ranking ability over all thresholds

PR-AUC (Precision-Recall Curve)

- **Precision**: $\frac{TP}{TP+FP}$
- Focuses on positive class (e.g. conflict); better under imbalance

F1 Score

$$\text{F1} = 2 \cdot \frac{\text{Precision} \cdot \text{Recall}}{\text{Precision} + \text{Recall}}$$

- Harmonic mean of precision and recall. Sensitive to false positives/negatives

Brier Score (BS)

$$BS = \frac{1}{N} \sum_{i=1}^{N} (P_i - O_i)^2$$

- Evaluates the accuracy of probabilistics.

Accuracy

Predictive Performance Across Models and Time Horizons

Table 1: Model performance k' months ahead ($k' = 1, 3, 6, 9$). Bold best, underlined second-best.

	PR-AUC % (↑)				ROC-AUC % (↑)				F1 Score % (↑)			
Model	1	3	6	9	1	3	6	9	1	3	6	9
ViEWS	36.4	32.8	31.0	29.9	94.8	92.2	90.4	88.6	34.7	31.4	29.6	28.8
XGBoost	37.4	33.1	30.8	30.1	93.9	93.1	92.4	91.6	35.4	31.4	28.7	27.3
RNN	33.4	29.7	29.1	28.6	92.1	91.6	91.4	91.3	35.7	33.6	32.4	31.9
GRU	35.8	31.5	30.2	29.9	92.2	91.3	91.0	90.8	39.5	36.4	35.8	35.4
LSTM	36.2	32.1	30.1	29.4	92.3	92.0	91.5	91.2	39.4	36.6	35.5	34.8
GCN	35.6	31.2	29.7	28.7	91.8	91.1	90.8	90.5	39.8	36.4	35.5	35.0
GAT	38.9	34.4	32.7	31.5	94.3	94.0	93.5	93.2	40.6	36.1	36.4	35.8
STSGCN	42.6	38.5	35.4	32.7	95.1	94.8	94.6	94.4	42.4	37.2	35.2	36.1
STGNN	43.3	39.2	35.4	31.9	95.2	95.0	94.6	93.9	42.5	38.3	36.1	35.9
GraphWaveNet	37.1	33.7	31.9	30.2	94.1	93.8	93.7	93.5	39.2	36.9	35.8	34.6
STGCN	40.3	35.8	33.2	31.5	94.5	94.3	94.0	93.8	41.1	36.0	36.1	35.8
ST-GCN	40.8	36.1	33.8	31.4	94.7	94.2	94.0	93.7	41.3	37.9	36.4	36.0
D2STGNN	44.8	39.6	35.7	32.6	95.6	95.0	94.5	94.2	42.7	38.9	36.2	35.9
ConflictNet	**56.7**	**51.2**	**48.8**	**47.6**	**97.0**	**96.6**	**96.3**	**96.2**	**53.7**	**50.0**	**48.2**	**47.5**

Did We Capture the Diffusion Process? -Ablation Study

Table 2: Performance Comparison in Ablation Study

	PR-AUC %(↑)	**ROC-AUC %(↑)**	**F1 %(↑)**
ConflictNet	56.7	97.0	53.7
w/o de-bias	53.4	96.7	50.6
w/o transfer	40.3	94.9	39.1

Notes: We forecast the 1st month ahead and perform 3-fold cross-validation. w/o causal is ConflictNet without De-bias Module. w/o transfer is ConflictNet without Transfer Module.

Did We Capture the Diffusion Process? -Spatial-Temporal Generalization

Table 3: Out-of-distribution performance of ConflictNet under spatial and temporal train-test splits. Despite substantial differences in conflict patterns across regions and periods, the model maintains high accuracy and recall, demonstrating strong generalization.

	Train	Test	PR-AUC %(↑)				ROC-AUC %(↑)				F_1 %(↑)			
			1	3	6	9	1	3	6	9	1	3	6	9
	*	*	56.7	51.2	48.8	47.6	97.0	96.6	96.3	96.2	53.7	50.0	48.2	47.5
Spatial	E of 20řE	W of 20řE	53.5	49.0	46.8	44.1	96.5	96.2	95.9	95.6	50.1	48.3	46.7	45.2
	W of 20řE	E of 20řE	53.8	49.2	46.7	43.3	96.5	96.1	95.8	95.6	50.3	48.5	46.2	44.7
	S of 12řN	N of 12řN	51.6	46.4	42.8	39.2	96.3	95.9	95.6	95.5	49.2	47.5	45.9	43.9
	N of 12řN	S of 12řN	45.4	39.9	34.5	31.6	95.6	95.1	95.4	95.0	43.3	39.4	35.8	34.3
Temporal	1990.1-2008.9	2008.10-2020.12	55.5	50.0	47.1	43.8	96.8	96.5	96.2	96.0	51.4	49.5	47.8	46.1
	1990.1-2012.12	2013.1-2020.12	53.2	51.2	48.5	42.7	96.6	96.3	96.0	95.8	50.1	48.3	46.6	44.9

Cases: Damascus

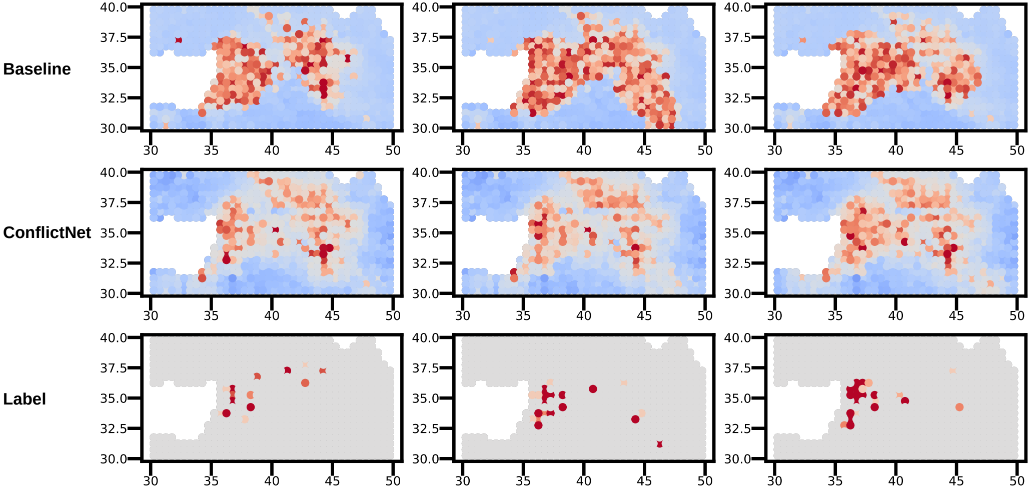

Figure 11: Predicted conflict factors (ConflictNet and baseline) and observed events in Damascus.

Interpretability

Heterogeneous:Define the Local Sensitivity of Diffusion Effect (LSD)

Key Assumptions and Expansion

- Assume the PDE parameter $LSD = u(x, y, t; D_0, \mu_0) - u_0(x, y, t)$.
- Expansion in feature space (D, μ):

$$LSD = \frac{\partial u}{\partial D} \cdot \Delta D + \frac{\partial u}{\partial \mu} \cdot \Delta \mu + o\left(\sqrt{\Delta D^2 + \Delta \mu^2}\right).$$

Proof Notes

Utilize Newton-Leibniz law, we can obtain

$$\frac{\partial}{\partial t}\frac{\partial u}{\partial \mu} = \frac{\partial}{\partial \mu}\frac{\partial u}{\partial t} = -\nabla(Fu).$$

$$\frac{\partial u(t, x, y; D_0, \mu_0)}{\partial \mu} = -\int_{t_0}^{t} \nabla(Fu_0(t, x, y))dt + \frac{\partial u(t_0, x, y; D_0, \mu_0)}{\partial \mu}.$$

Interpretable Sensitivity: ParVul Index

ParVul Index (Policy-Affected Relative Vulnerability)

$$\boxed{\mathsf{ParVul}_{\mathbf{w}}(t,x,y) = \frac{w_D \partial_D u + w_\mu \partial_\mu u}{u + \varepsilon}}$$

Analytical properties

- ParVul is *first-order accurate*. Predicts outcome change under small interventions almost exactly.
- Linearity and Composability. ParVul supports vectorized, interpretable policy mixes.
- Shift-Scale Robustness. textbfClaim: Increasing $u \to u + c$ scales ParVul downward.

$$\mathrm{ParVul}' = \frac{u}{u + c + \varepsilon} \, \mathrm{ParVul}$$

Captures buffer effect higher baseline = lower sensitivity.

Sensitivity on Excluded Ethnic Groups (Time)

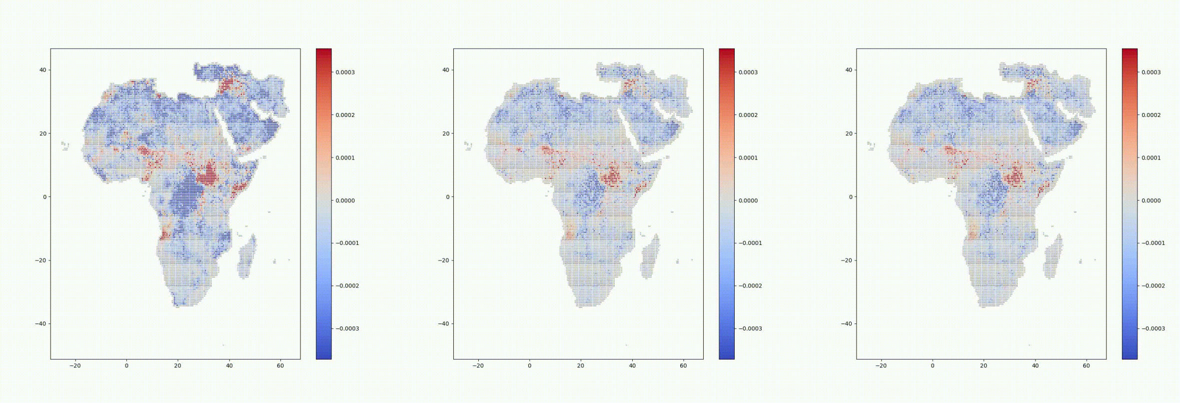

Figure 12: Sensitivity on Excluded Ethnic Groups (2008.3-2010.3)

Sensitivity on Orders

Self | First order neighborhood | Second order neighborhood

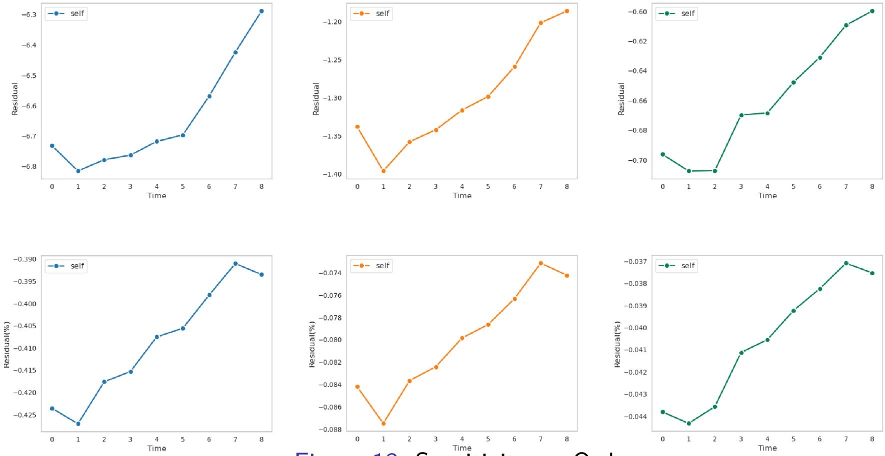

Figure 13: Sensitivity on Orders

What specific factors drive the spatial diffusion of intrastate conflict?

Empirical Question

- Opportunity and grievance are traditionally treated as exogenous drivers. (Cederman et al., 2011; Fearon and Laitin, 2003)
- However, these mechanisms embedded in the **spatiotemporal process** of political violence. (Buhaug and Gleditsch, 2008; Cederman et al., 2013a,b)
- Disentangling the specific contributions of these mechanisms to the diffusion patterns of intrastate conflict presents a significant challenge. (Ward et al., 2013; Weidmann, 2015)

- **Research Question:** What specific factors, and what forms of interaction among them, drive the spatial diffusion of intrastate conflict?

Factors Driving the Spread

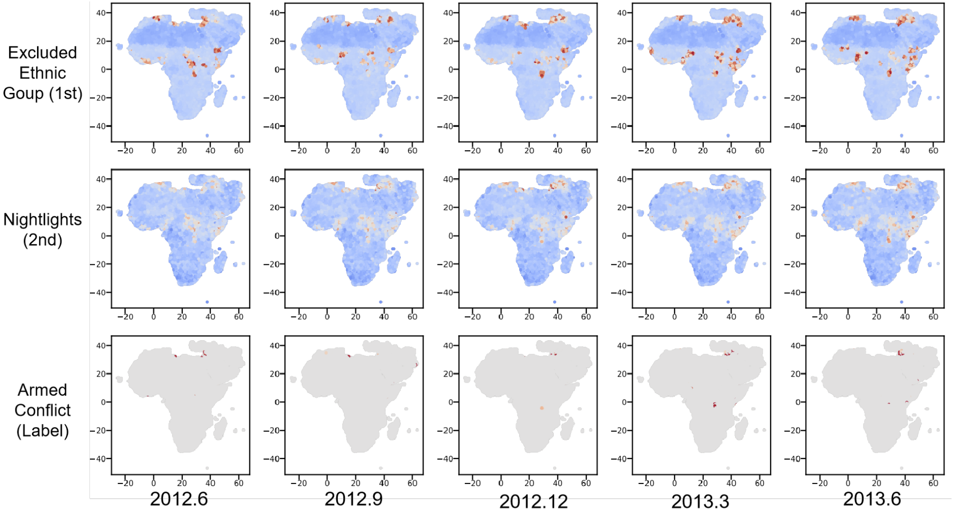

Figure 14: Feature Importance in Modeling Armed Conflict Spreading

Discussion

- We propose a **physics-informed deep learning framework** for modeling armed conflict dynamics.
- Our model achieves a **56% improvement in predictive accuracy** over ViEWS on high-resolution PRIO-GRID data, outperforming leading machine learning baselines.
- We offer a **generalizable modeling approach** bridging computational techniques and political science theory, applicable to other diffusion phenomena such as protest, migration, and epidemics.

References I

Bertozzi, A. L., Short, M. B., Brantingham, P. J., Sgourakis, G., and Tita, G. (2010). A pde model for criminal behavior. *SIAM Journal on Applied Mathematics*, 70(6):1984–2006.

Brandt, P. T., DOrazio, V., Khan, L., Li, Y.-F., Osorio, J., and Sianan, M. (2022). Conflict forecasting with event data and spatio-temporal graph convolutional networks. *International Interactions*, 48(4):800–822.

Brockmann, D. and Helbing, D. (2013). The hidden geometry of complex, network-driven contagion phenomena. *Science*, 342(6164):1337–1342.

Buhaug, H. and Gleditsch, K. S. (2008). Contagion or confusion? why conflicts cluster in space. *International studies quarterly*, 52(2):215–233.

Cederman, L.-E., Gleditsch, K. S., and Buhaug, H. (2013a). *Inequality, grievances, and civil war*. Cambridge University Press.

Cederman, L.-E., Gleditsch, K. S., Salehyan, I., and Wucherpfennig, J. (2013b). Transborder ethnic kin and civil war. *International Organization*, 67(2):389410.

Cederman, L.-E. and Weidmann, N. B. (2017). Predicting armed conflict: Time to adjust our expectations? *Science*, 355(6324):474–476.

Cederman, L.-E., Weidmann, N. B., and Gleditsch, K. S. (2011). Horizontal Inequalities and Ethnonationalist Civil War: A Global Comparison. *American Political Science Review*, 105(3):478–495.

Chadefaux, T. (2022). A shape-based approach to conflict forecasting. *International Interactions*, 48(4):633–648.

Couzin, I. D., Krause, J., Franks, N. R., and Levin, S. A. (2005). Effective leadership and decision-making in animal groups on the move. *Nature*, 433(7025):513–516.

Dando, B. D. E., Goertz-Allmann, B. P., Brissaud, Q., Köhler, A., Schweitzer, J., Kværna, T., and Liashchuk, A. (2023). Identifying attacks in the russiaukraine conflict using seismic array data. *Nature*, 621(7980):767–772.

Epstein, J. M. (2002). Modeling civil violence: An agent-based computational approach. *Proceedings of the National Academy of Sciences*, 99(suppl 3):7243–7250.

Fearon, J. D. and Laitin, D. D. (2003). Ethnicity, Insurgency, and Civil War. *American Political Science Review*, 97(01):75–90.

Galam, S. (1997). Rational group decision making: A random field ising model at t=0. *Physica A: Statistical Mechanics and its Applications*, 238(1-4):66–80.

Hegre, H., Allansson, M., Basedau, M., Colaresi, M., Croicu, M., Fjelde, H., Hoyles, F., Hultman, L., Högbladh, S., Jansen, R., Mouhleb, N., Muhammad, S. A., Nilsson, D., Nygård, H. M., Olafsdottir, G., Petrova, K., Randahl, D., Rød, E. G., Schneider, G., Von Uexkull, N., and Vestby, J. (2019). ViEWS: A political violence early-warning system. *Journal of Peace Research*, 56(2):155–174.

References II

Hegre, H., Bell, C., Colaresi, M., Croicu, M., Hoyles, F., Jansen, R., Leis, M. R., Lindqvist-McGowan, A., Randahl, D., Rød, E. G., and Vesco, P. (2021). ViEWS $_{2020}$: Revising and evaluating the ViEWS political Violence Early-Warning System. *Journal of Peace Research*, 58(3):599–611.

Hegre, H., Metternich, N. W., Nygård, H. M., and Wucherpfennig, J. (2017). Introduction: Forecasting in peace research. *Journal of Peace Research*, 54(2):113–124.

Hegre, H., Vesco, P., and Colaresi, M. (2022). Lessons from an escalation prediction competition. *International Interactions*, 48(4):521–554.

Helbing, D. (2001). Traffic and related self-driven many-particle systems. *Reviews of Modern Physics*, 73(4):1067–1141.

Holmes, E. E. (1993). Are diffusion models too simple? a comparison with telegraph models of invasion. *The American Naturalist*, 142(5):779–795.

Krapivsky, P. L., Redner, S., and Ben-Naim, E. (2010). *A Kinetic View of Statistical Physics*. Cambridge University Press, Cambridge, UK.

Lindholm, A., Hendriks, J., Wills, A., and Schön, T. B. (2022). Predicting political violence using a state-space model. *International Interactions*, 48(4):759–777.

Muchlinski, D., Siroky, D., He, J., and Kocher, M. (2016). Comparing Random Forest with Logistic Regression for Predicting Class-Imbalanced Civil War Onset Data. *Political Analysis*, 24(1):87–103.

Nicolas, A. and Hassan, F. H. (2023). Social groups in pedestrian crowds: review of their influence on the dynamics and their modelling. *Transportmetrica A: Transport Science*.

O'Loughlin, J., Witmer, F. D. W., Linke, A. M., and Thorwardson, A. (2010). The locational determinants of civil war violence: Evidence from african conflicts. *Political Geography*, 29(8):638–648.

Orlova, E. V. (2024). A novel brillouin and langevin functions dynamic model for two conflicting social groups: Study of r&d processes. *Mathematics*, 12(17):2788.

Porter, M. A. and Gleeson, J. P. (2016). *Dynamical Systems on Networks: A Tutorial*, volume 4 of *Frontiers in Applied Dynamical Systems: Reviews and Tutorials*. Springer.

Radford, B. J. (2022). High resolution conflict forecasting with spatial convolutions and long short-term memory. *International Interactions*, 48(4):739–758.

Wang, Y. (2019). Comparing Random Forest with Logistic Regression for Predicting Class-Imbalanced Civil War Onset Data: A Comment. *Political Analysis*, 27(1):107–110.

References III

Ward, M. D., Metternich, N. W., Dorff, C. L., Gallop, M., Hollenbach, F. M., Schultz, A., and Weschle, S. (2013). Learning from the Past and Stepping into the Future: Toward a New Generation of Conflict Prediction. *International Studies Review*, 15(4):473–490.

Weidmann, N. B. (2015). Communication networks and the transnational spread of ethnic conflict. *Journal of peace research*, 52(3):285–296.

Zammit-Mangion, A., Dewar, M., Kadirkamanathan, V., and Sanguinetti, G. (2012). Point process modelling of the Afghan War Diary. *Proceedings of the National Academy of Sciences*, 109(31):12414–12419.

Zhang, Y., Long, M., Chen, K., Xing, L., Jin, R., Jordan, M. I., and Wang, J. (2023). Skilful nowcasting of extreme precipitation with NowcastNet. *Nature*, 619(7970):526–532.

Appendix

Optimizing D and μ: A Perspective Embedded in Network (1)

We assume the PDE parameter of u_0 is just (D_0, μ_0), i.e.

$$u_0(x, y, t) = u(x, y, t; D_0, \mu_0).$$

Then we have that under some regular conditions, $u(t, x, y; D_0 + \Delta D, \mu_0 + \Delta\mu)$ equals

$$u_0(t, x, y) + \frac{\partial u}{\partial D}\Big|_{(D,\mu,t)=(D_0,\mu_0,t)} \cdot \Delta D + \frac{\partial u}{\partial \mu}\Big|_{(D,\mu,t)=(D_0,\mu_0,t)} \cdot \Delta\mu + o(\sqrt{|\Delta D|^2 + |\Delta\mu|^2}).$$

Also, in PDE, we can change the order of the deviation

$$\frac{\partial}{\partial t}\frac{\partial u}{\partial D} = \frac{\partial}{\partial D}\frac{\partial u}{\partial t} = \nabla^2 u.$$

Optimizing D and μ: A Perspective Embedded in Network (2)

Utilize Newton-Leibniz law, we can obtain

$$\frac{\partial u(t,x,y;D_0,\mu_0)}{\partial D} = \int_{t_0}^{t} \nabla^2 u_0(x,y,t)dt + \frac{\partial u(t_0,x,y;D_0,\mu_0)}{\partial D}.$$

Similarly, we can obtain that

$$\frac{\partial}{\partial t}\frac{\partial u}{\partial \mu} = \frac{\partial}{\partial \mu}\frac{\partial u}{\partial t} = -\nabla(Fu).$$

and

$$\frac{\partial u(t,x,y;D_0,\mu_0)}{\partial \mu} = -\int_{t_0}^{t} \nabla(Fu_0(t,x,y))dt + \frac{\partial u(t_0,x,y;D_0,\mu_0)}{\partial \mu}.$$

Optimizing D and μ: A Perspective Embedded in Network (3)

Therefore

$$
\begin{aligned}
& u(t,x,y;D_0+\Delta D,\mu_0+\Delta\mu) \\
=& u_0(t,x,y) + \frac{\partial u}{\partial D}\Big|_{(D,\mu,t)=(D_0,\mu_0,t)} \cdot \Delta D + \frac{\partial u}{\partial \mu}\Big|_{(D,\mu,t)=(D_0,\mu_0,t)} \cdot \Delta\mu + o(\sqrt{|\Delta D|^2+|\Delta\mu|^2}) \\
=& u_0(t,x,y) - u_0(t_0,x,y) + \left(\int_{t_0}^{t} \nabla^2 u_0(t,x,y)dt\right)\Delta D - \left(\int_{t_0}^{t} \nabla(F(x,y)u_0(t,x,y))dt\right)\Delta\mu \\
& + \left\{u_0(t_0,x,y) + \frac{\partial u(t_0,x,y;D_0,\mu_0)}{\partial D}\Delta D + \frac{\partial u(t_0,x,y;D_0,\mu_0)}{\partial \mu}\Delta\mu\right\} + o(\sqrt{|\Delta D|^2+|\Delta\mu|^2}) \\
=& u_0(t,x,y) - u_0(t_0,x,y) + \left(\int_{t_0}^{t} \nabla^2 u_0(t,x,y)dt\right)\Delta D - \left(\int_{t_0}^{t} \nabla(F(x,y)u_0(t,x,y))dt\right)\Delta\mu \\
& + u(t_0,x,y;D_0+\Delta D,\mu_0+\Delta\mu) + o(\sqrt{|\Delta D|^2+|\Delta\mu|^2}).
\end{aligned}
$$

Optimizing D and μ: A Perspective Embedded in Network (4)

Here we choose $t_0 = \tau(x, y)$ such that for any $(D, \mu) \in \mathcal{B}((D_0, \mu_0), r)$,

$$u(\tau(x, y), x, y; D, \mu) \equiv 0.$$

Then we have that

$$\begin{aligned} & u(t, x, y; D_0 + \Delta D, \mu_0 + \Delta\mu) \\ \approx & u_0(t, x, y) - u_0(t_0, x, y) + \left(\int_{t_0}^{t} \nabla^2 u_0(t, x, y) dt \right) \Delta D - \left(\int_{t_0}^{t} \nabla (F(x, y) u_0(t, x, y)) dt \right) \Delta\mu, \end{aligned}$$

and the error term is $o(\sqrt{|\Delta D|^2 + |\Delta\mu|^2})$.